CHAPTER IV
TEST RESULTS

In this chapter, the results of the monotonic tensile, compressive and cyclic tests are presented.

4.1 Monotonic tensile test results

4.1.1 Effect of slip and deformation of threads at connections between coupler and threaded bars

In order to determine the amount of deformations of threads in the threaded bars and the coupler, the tensile test result of the specimen T4.0-G30 is conducted. The deformation of the coupler gap is compared to the total deformation of the coupler and lock nut as illustrated in Figure 4.2. The difference is 0.49 mm which is equal to the sum of deformations of threads.

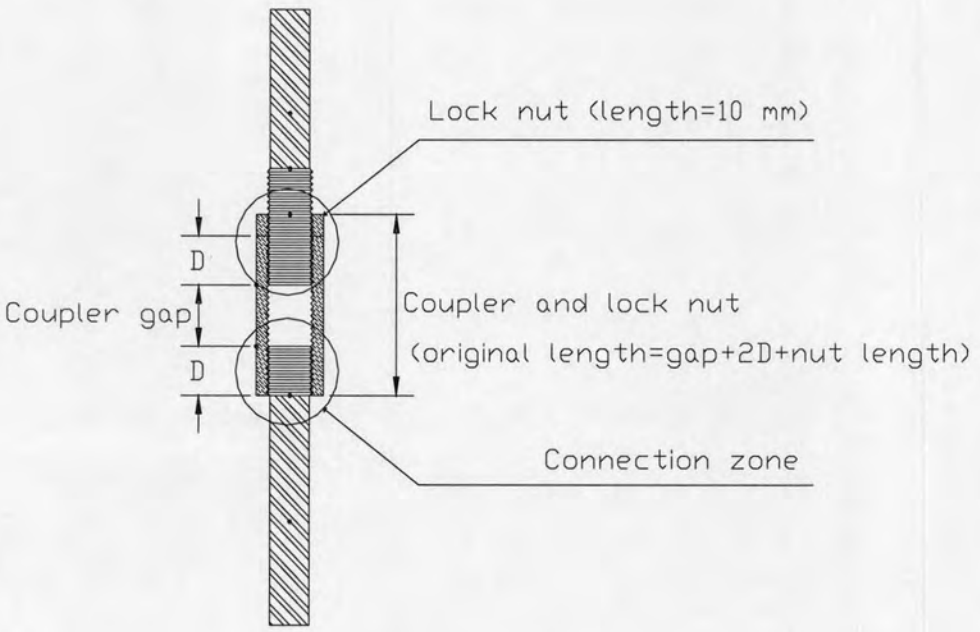

Figure 4.1 Connection zones of threaded coupler and bars

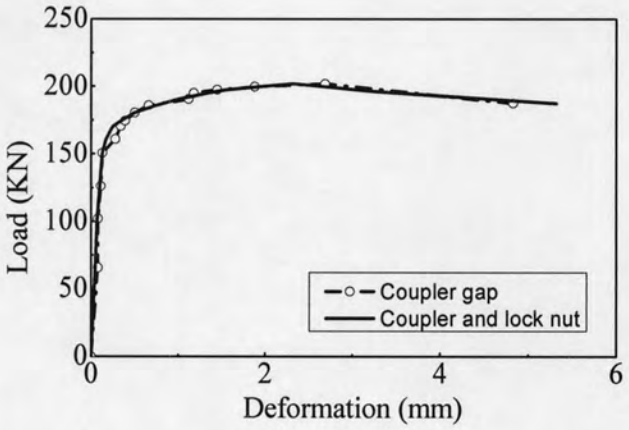

Figure 4.2 Comparison of deformations of coupler gap and total of coupler and lock nut

The effect from the slip between the threaded coupler and threaded bars is illustrated in Figure 4.3. Another variable affecting the actual behavior of mechanical splice is the reduction of the cross sectional area of the bar in the threaded zones. All of the mentioned variables also influence the stiffness of mechanical splice to be smaller than the stiffness at the lower bar; the upper bar and thread; the coupler and lock nut as depicted in Figure 4.4.

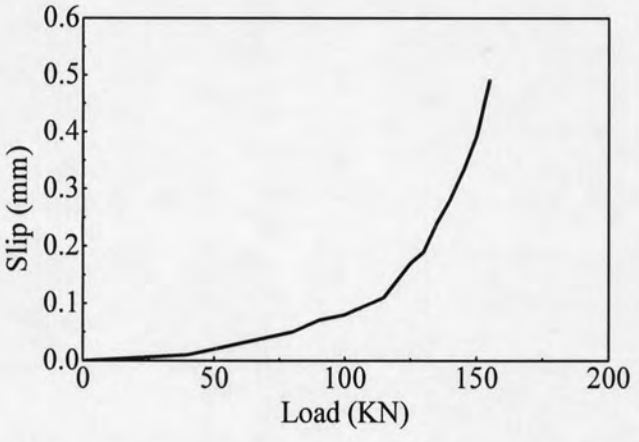

Figure 4.3 Slip-load relation of specimen T4.0-G30

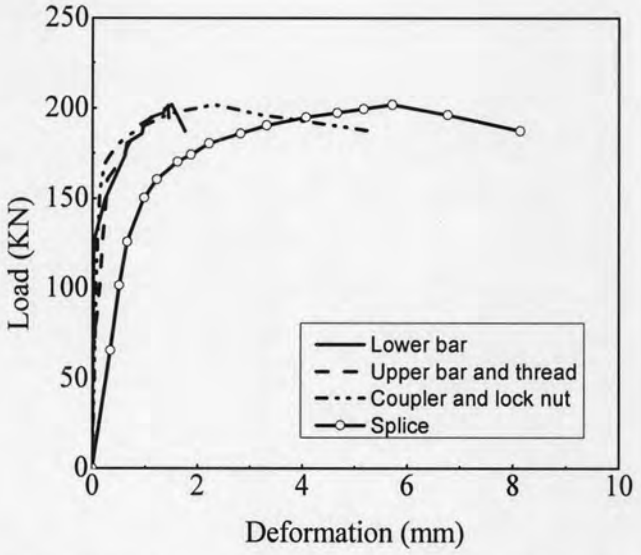

Figure 4.4 Load-deformation relation of the mechanical splice and its component (Specimen T4.0-G30)

4.1.2 Effect of coupler thickness

To find out the optimal mechanical splice that allows failure to occur at the coupler with the largest elongation. The tensile behavior of the mechanical splice specimen with variation of thickness was investigated from Figure 4.5, it could be observed that as the thickness of the coupler increases, the strength of the splice also increases. The difference in the deformation depends on both thickness and coupler gap length. Figure 4.5 also indicates that the variation of the coupler thickness from 3.0 to 4.0 mm tend to increase both strength and deformation. The two specimens fail at the coupler as depicted in Figure 4.6. However, the coupler with a thickness of 4.5 mm has higher strength but less deformation as well as energy dissipation, as shown in Figure 4.7. This is because the higher strength of coupler than the strength of threaded bars, leads to a smaller elongation of coupler, as shown in Figure 4.8. In addition, the bar fails for the specimen T4.5-G30 as shown in Figure 4.6.

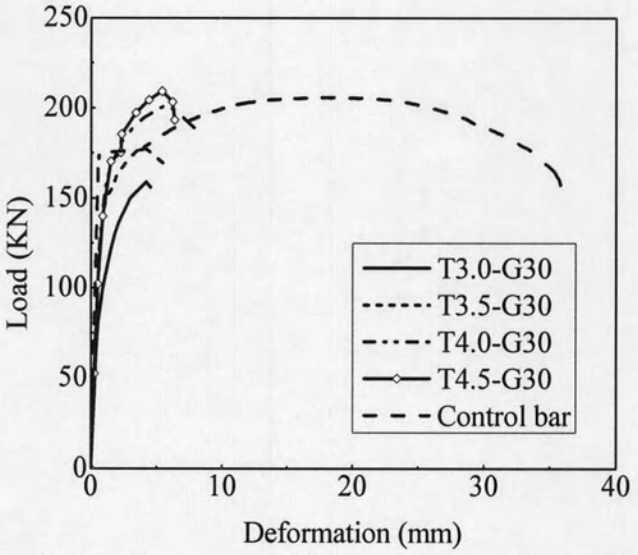

Figure 4.5 Load-deformation of control bar and mechanical splice specimens with different coupler thicknesses

Figure 4.6 Failure modes of specimens

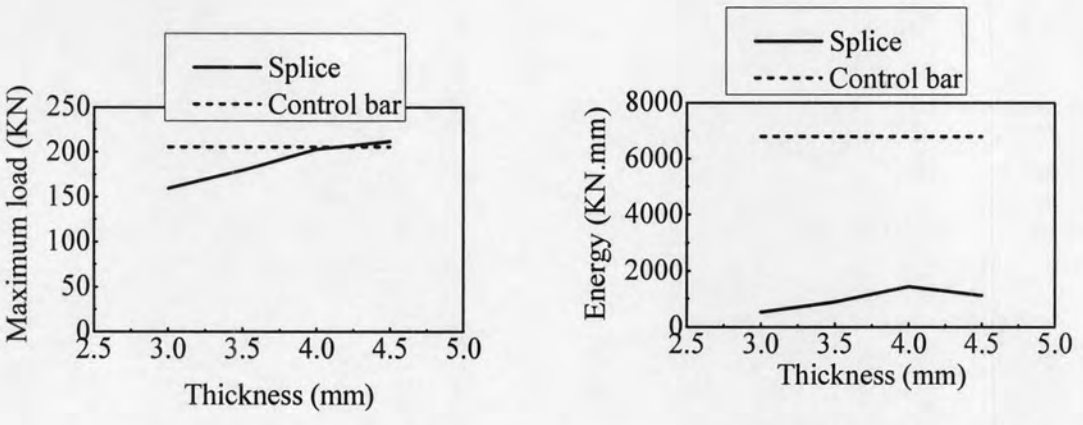

(a) Maximum Load (b) Energy Dissipation

Figure 4.7 Comparison of maximum load and energy dissipation for different coupler thicknesses

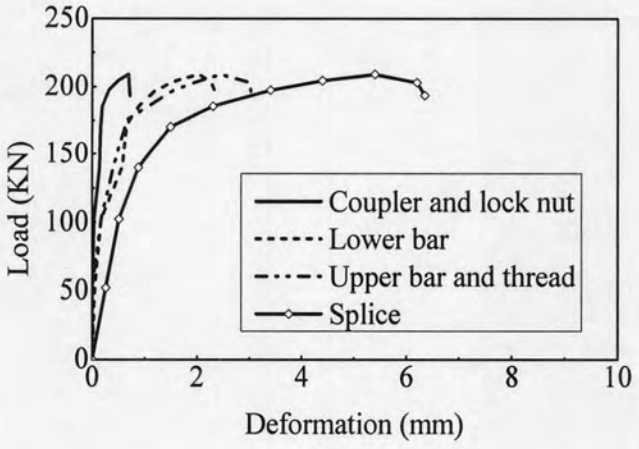

Figure 4.8 Load-deformation of the mechanical splice T4.5-G30 and its components

Figure 4.9 illustrates that the stiffness of the mechanical splice is less than that of the control bar. It should be noted that the specimen T3.0-G30 has smallest coupler thickness (3.0 mm) as well as the smallest coupler area (315.40 mm^2), leading to the lowest stiffness.

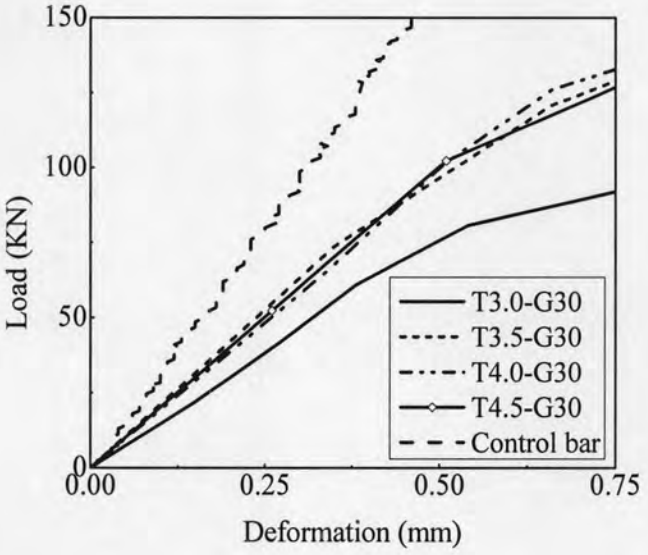

Figure 4.9 Stiffness of mechanical splices and control bar

The variation of energy dissipation of the coupler gap due to the changes of coupler thicknesses is presented in Figure 4.10 (a). The gauge lengths of the coupler gap and mechanical splice shows in Figure 4.11. It could be observed in Figure 4.10 (a) that the energy dissipation of the coupler gap increases when the thickness increases from 3.0 mm to 4.0 mm. For a thickness of 4.5 mm, the energy dissipation decreases. The energy dissipation of the coupler gaps normalized to the total energy of the mechanical splices as shown in Figure 4.12. The normalized energy increases when the thickness is increased from 3.0 mm to 3.5 mm and decreases when the thickness increases from 3.5 mm to 4.5 mm.

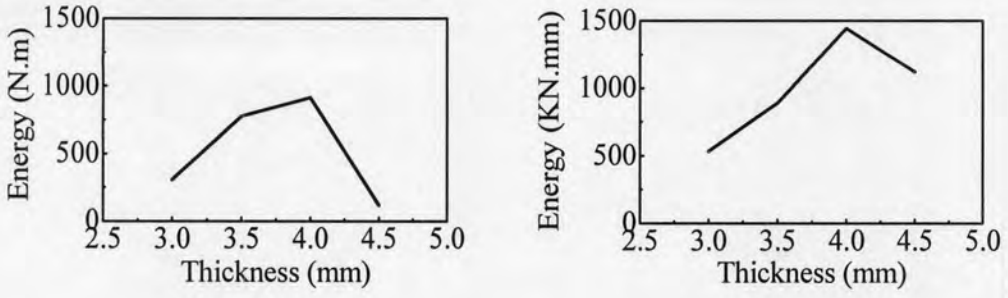

(a) Coupler gap (b) Mechanical splice

Figure 4.10 Variation of energy dissipation of the coupler gaps and mechanical splices due to different coupler thicknesses

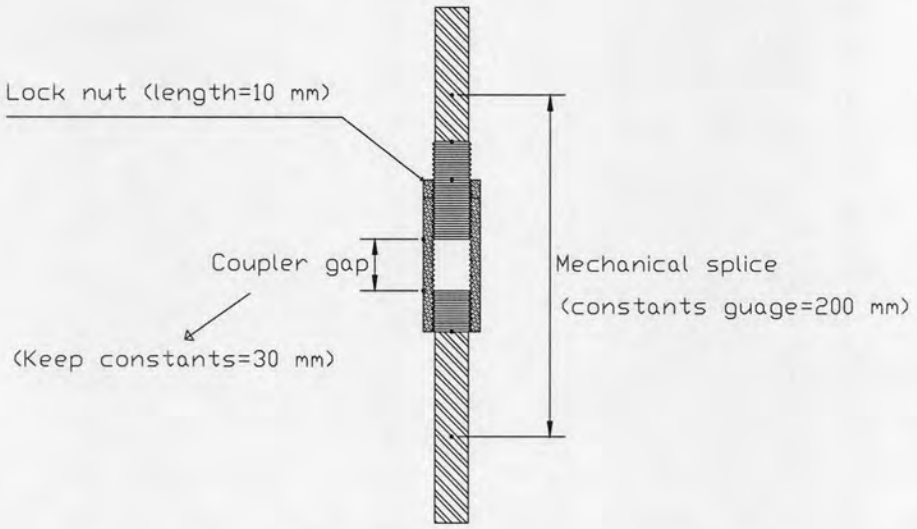

Figure 4.11 Gauge lengths of the coupler gap and mechanical splice

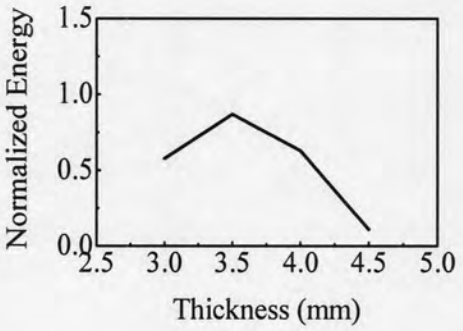

Figure 4.12 Variation of normalized energy of the coupler gap due to different coupler thicknesses

Therefore, two specimens with thicknesses of 4.0 and 3.5 mm will be investigated for various coupler gaps.

4.1.3 Effect of coupler gap length

To evaluate the ductility as well as energy dissipation of the mechanical splices, the tensile behavior of the mechanical splice specimens with various coupler gap lengths was investigated. The results are shown in Figures 4.13 and 4.14 for thicknesses of 4.0 and 3.5 mm, respectively. It can be observed that the elongation of splices increases when the coupler gap length increases. On the other hand, the maximum load is more or less the same. The stiffness of splices is smaller than that of

the control bar as shown in Figures 4.15 and 4.16. Figure 4.17 illustrates the failure modes of all specimens. All specimens fail in tension rupture of couplers.

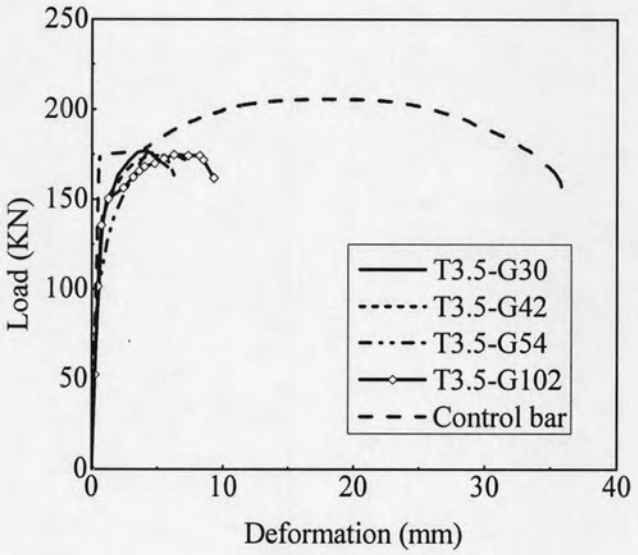

Figure 4.13 Load-deformation of control bar and mechanical splices with different coupler gap lengths (t = 3.5 mm)

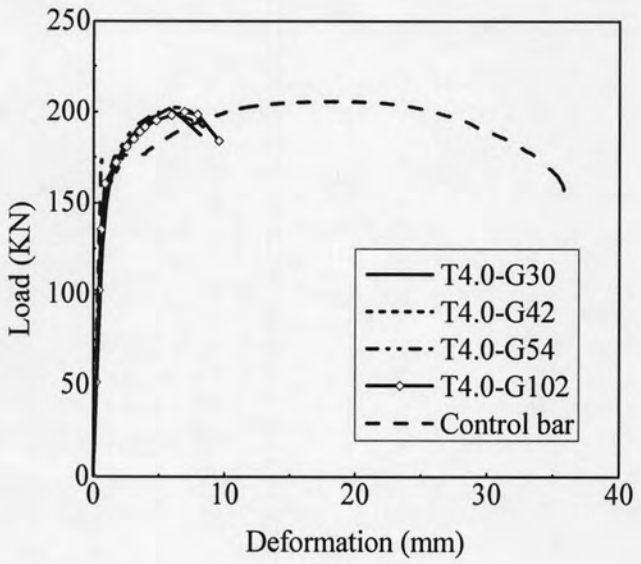

Figure 4.14 Load-deformation of control bar and mechanical splices with different coupler gap lengths (t = 4.0 mm)

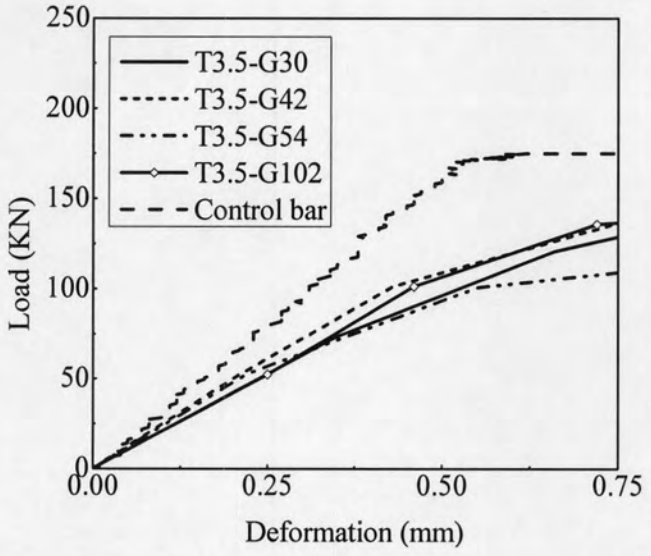

Figure 4.15 Stiffness of control bar and mechanical splices with different coupler gap lengths (t = 3.5 mm)

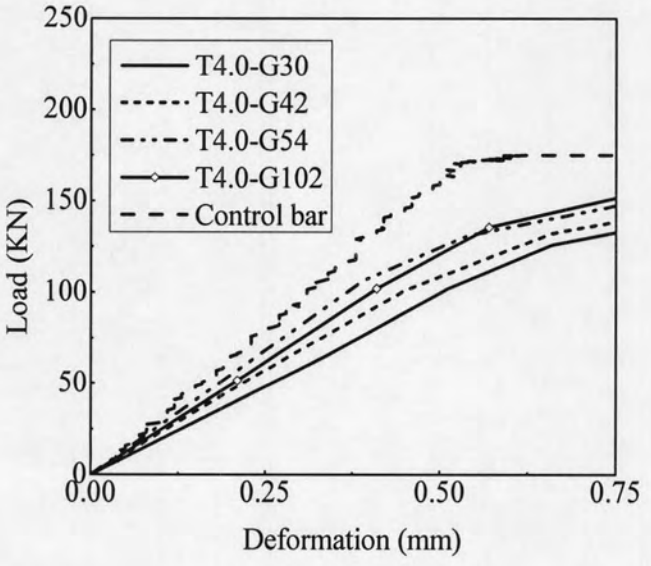

Figure 4.16 Stiffness of control bar and mechanical splices with different coupler gap lengths (t = 4.0 mm)

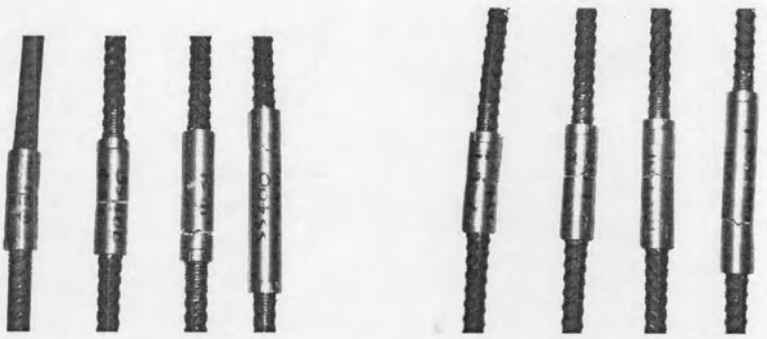

(a) Specimens with 3.5 mm thick (b) Specimens with 4.0 mm thick

Figure 4.17 Failure modes of mechanical splice specimens with 4.0 mm and 3.5 mm thick

The comparison of mechanical splices with various coupler gaps and thicknesses is presented in Figure 4.18. The strength of specimens with a thickness of 3.5 mm is smaller than the yield load of rebars. As shown in Figure 4.18, the final deformation of specimens with a coupler thickness of 3.5 mm is smaller than that with a coupler thickness of 4.0 mm. The maximum load and energy dissipation are summarized in Figure 4.19. The specimens with a coupler thickness of 4.0 mm have larger energy dissipation.

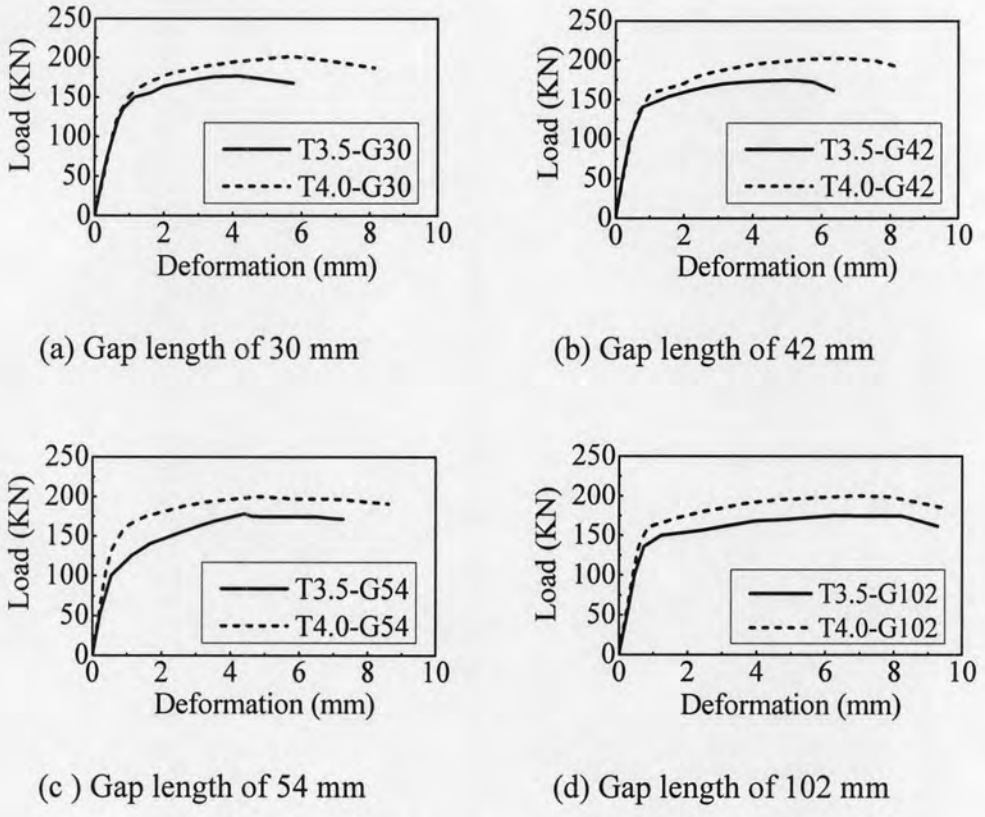

(a) Gap length of 30 mm

(b) Gap length of 42 mm

(c) Gap length of 54 mm

(d) Gap length of 102 mm

Figure 4.18 Comparison of load-deformation curves of mechanical splices with different coupler thicknesses and coupler gap lengths

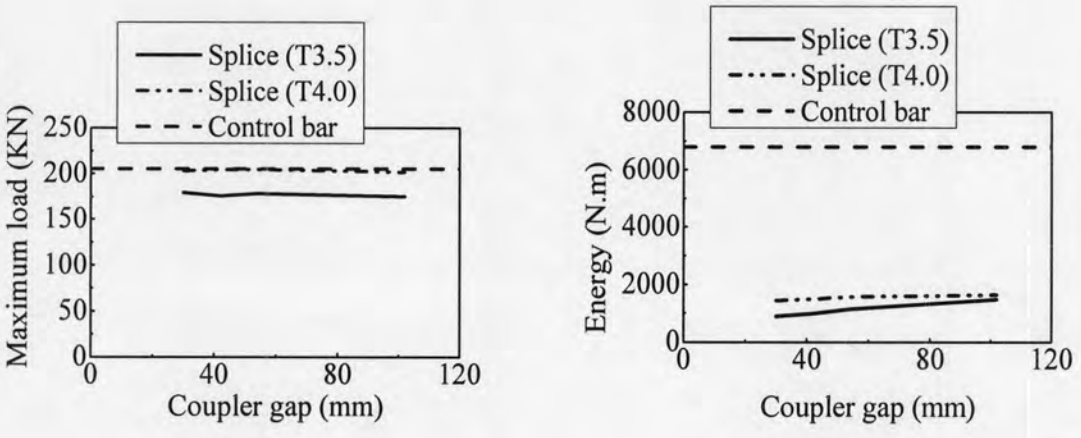

(a) Maximum load

(b) Energy dissipation

Figure 4.19 Comparison of maximum load and energy dissipation for control bar and mechanical splice specimens with different coupler gap lengths

The energy dissipation of coupler gaps normalized to the total energy of splices is presented in Figure 4.20 (b). It is obvious that as the gap length increases, the energy dissipation increases.

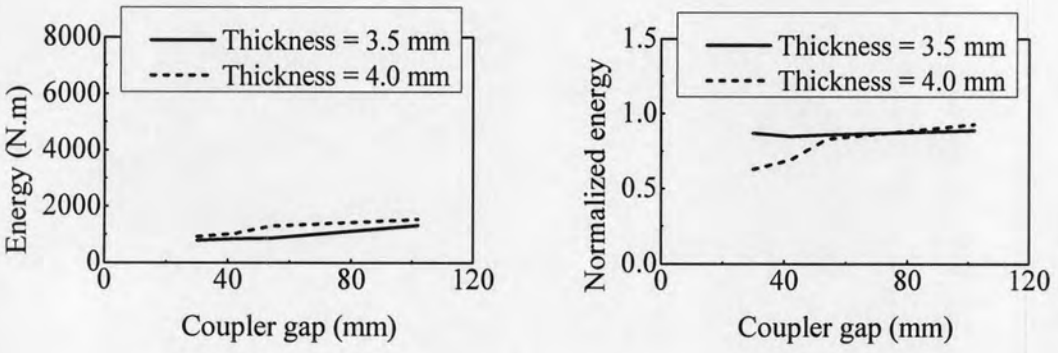

(a) Energy dissipation (b) Normalized energy dissipation

Figure 4.20 Variation of energy dissipation and normalized energy dissipation for the different coupler gap lengths

4.2 Monotonic compressive test results

4.2.1 Test results

The splices with a coupler thickness of 4.0 mm and various gap lengths were subjected to monotonic compressive test. The load-deformation relations are shown in Figure 4.21. The maximum load of the control bar is 188.42 kN and the load drops sharply after buckling. The splices have larger loads and ductility.

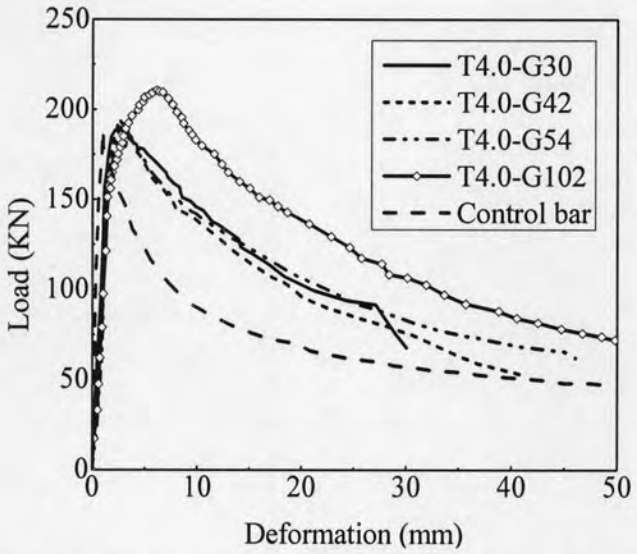

Figure 4.21 Load-deformation relation of control bar and mechanical splices at different coupler gap lengths

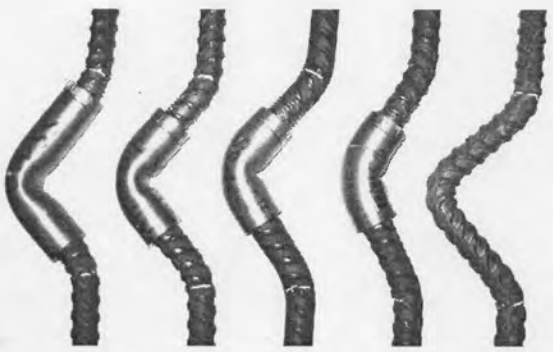

Figure 4.22 Failure modes of mechanical splice specimens under compression test

For quantitative comparison of the energy dissipation of the mechanical splices and control bar, the energy dissipation of each specimen is evaluated at the load dropped by 20% from the peak load. Figure 4.23 shows the load-deformation relation at the state. It is found that the energy dissipation of the splice with a coupler gap length of 102 mm is 4.88 times the energy dissipation of the plain bar. The maximum load capacity of the splice is greater than that of the plain bar by 11.8%. The comparison of other splice specimens is illustrated in Figure 4.24. Table 4.1 tabulates the amount of energy dissipation and maximum load capacity of all specimens.

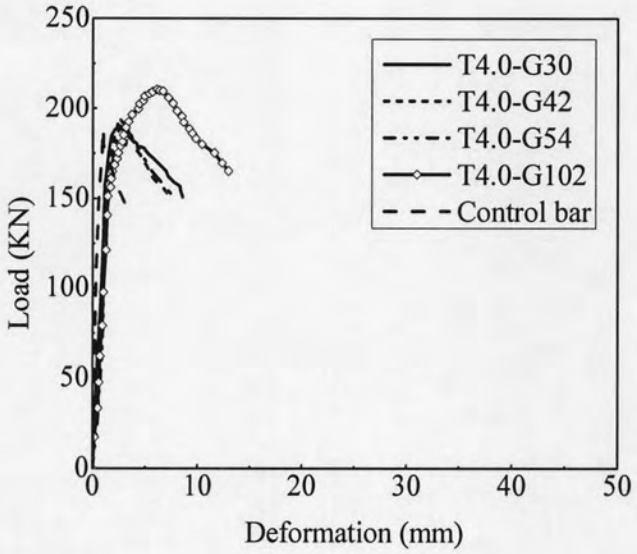

Figure 4.23 Load-deformation relation of control bar and mechanical splices at dropped load from the peak load about 20%

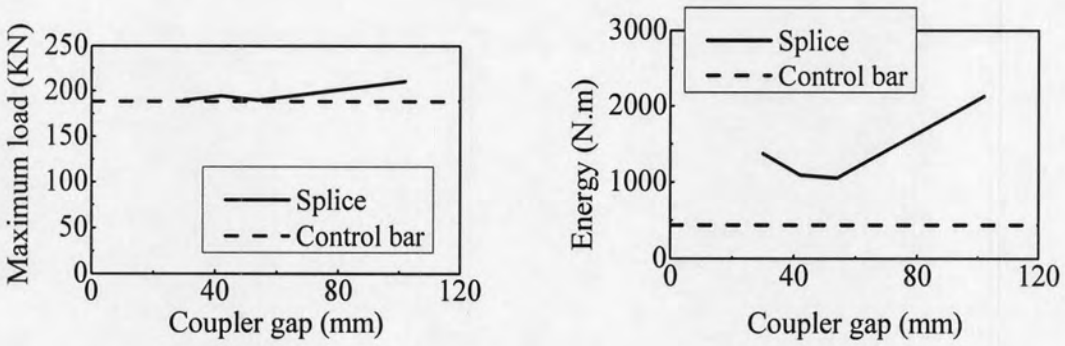

(a) Maximum Load

(b) Energy dissipation

Figure 4.24 Comparison of maximum load capacity and energy dissipation between control bar and mechanical splice specimens at different coupler gap lengths

Table 4.1 Summary of energy dissipation and maximum load capacity of specimens under compression test

Energy Dissipation (Nm)				Maximum Load Capacity (KN)		
Splice		Control Bar	Splice/Bar	Splice	Control Bar	Difference
Gap	Thickness (mm)			Thickness (mm)		(%)
(mm)	4.0			4.0		
30	1373.77	436.78	3.14	190.10	188.42	0.90
42	1093.91		2.50	194.54		3.26
54	1054.24		2.41	189.66		0.67
102	2130.50		4.88	210.59		11.78

Table 4.2 illustrates the deformed shapes of the specimens at various displacements. It is seen that lateral deformation of the mechanical splices is smaller compared to the control bar at the same level of deformation.

Table 4.2 Comparison of deformed shapes of compressive control bar and mechanical splice specimens at various stages

δ	Deformed shapes				
(mm)	CB-com	T4.0-G30-com	T4.0-G42-com	T4.0-G54-com	T4.0-G102-com
0					
5					
10		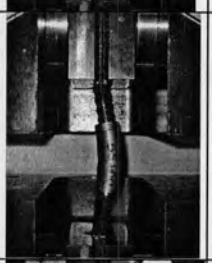			
15			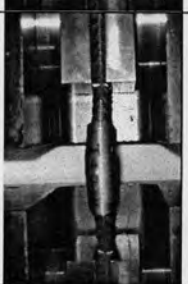		Not available
20					

25				Not available	
30					
40		End			
45		End	End		

4.3 Cyclic loading test

The cyclic loading test was conducted on a plain bar using the procedure explained in Section 3.5 in Chapter 3. The load-deformation relation is obtained as shown in Figure 4.25. It is seen that the hysteretic is biased to the compression side because of the slip between the bar and grips. The prescribed displacement of actuator stroke is not the actual displacement. As in tension, the specimen is undergoing smaller displacement than the prescribed displacement. In compression side the specimen also deformed smaller than the prescribed value. It could be observed during the test that the displacement is cumulative to compression side, leads to an unsymmetrical hysteretic curve. Figures 4.26-4.29 compare the hysteretic curves of

control bar and mechanical splice specimen at the variation of coupler gap lengths. It could be observed that the cyclic energy dissipation is increased as the coupler gap length is increased.

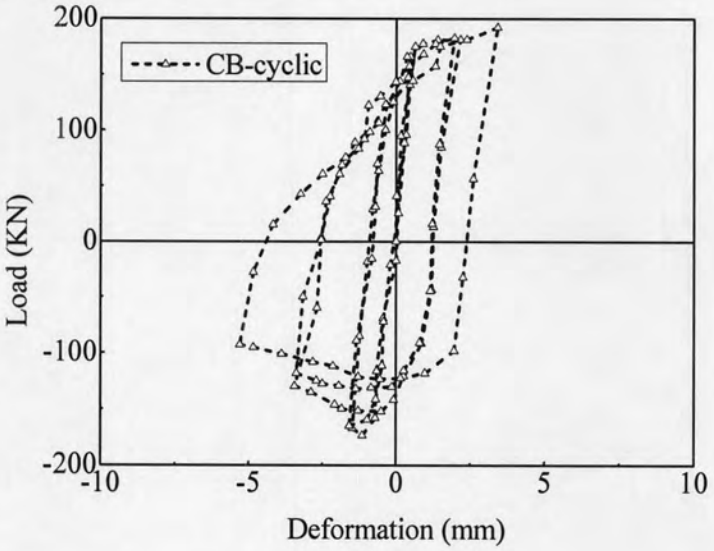

Figure 4.25 Load-deformation curve of control bar

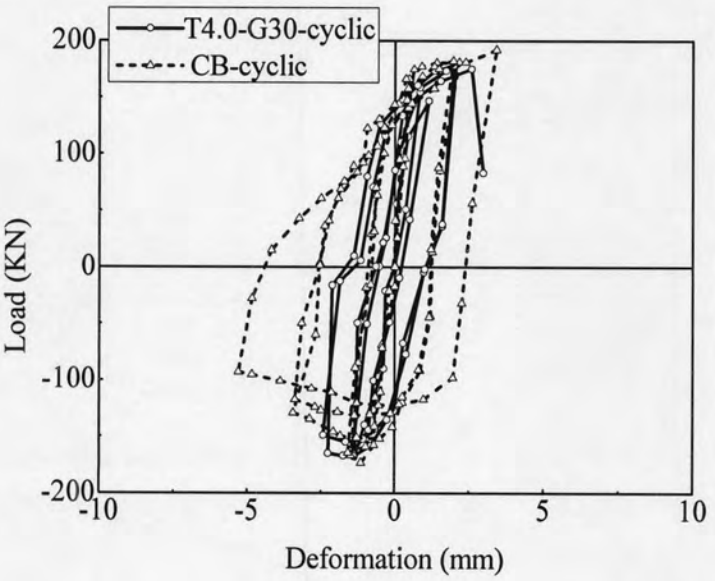

Figure 4.26 Comparison of load-deformation curve of control bar and mechanical splice T4.0-G30-cyclic

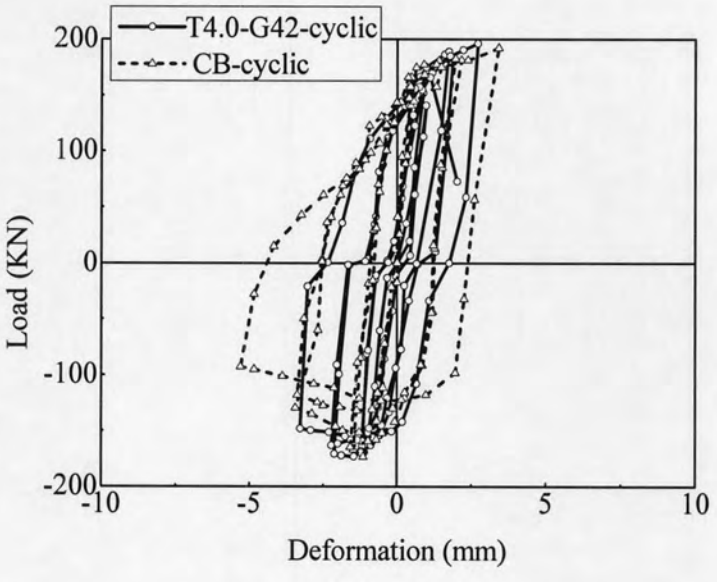

Figure 4.27 Comparison of load-deformation curve of control bar and mechanical splice T4.0-G42-cyclic

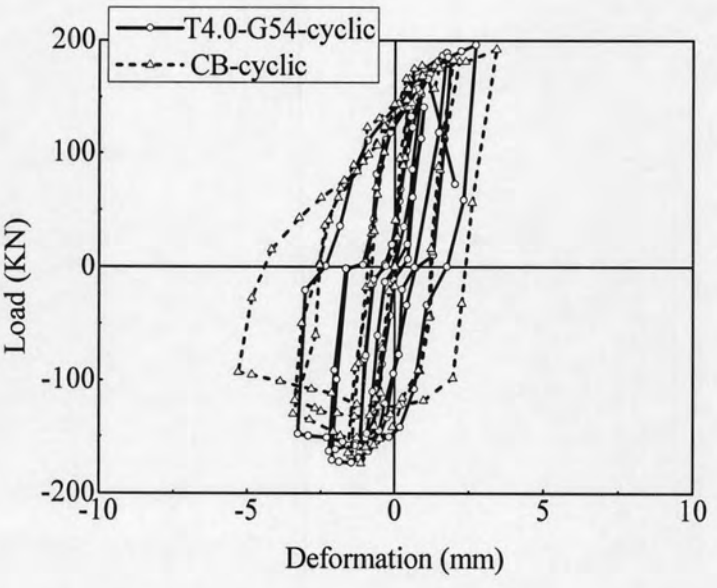

Figure 4.28 Comparison of load-deformation curve of control bar and mechanical splice T4.0-G54-cyclic

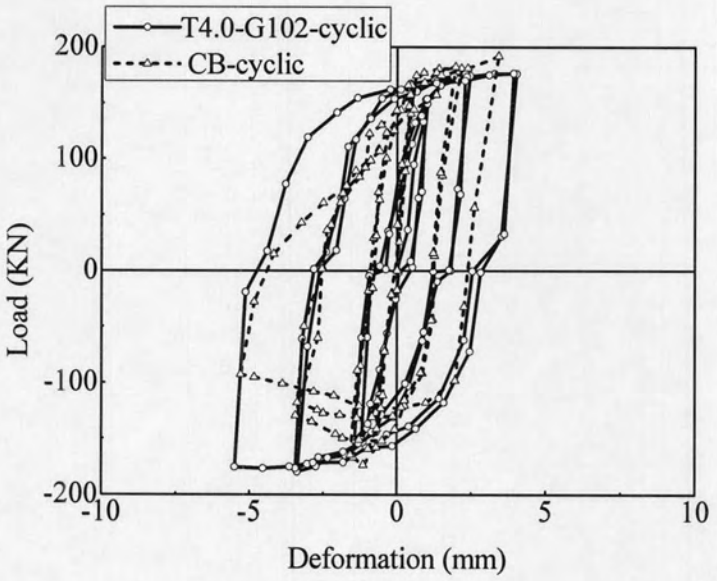

Figure 4.29 Comparison of load-deformation curve of control bar and mechanical splice T4.0-G102-cyclic